Journal of Korean Magnetics Society, Volume 5, Number 5, October 1995

MAGNETISM OF NANOPHASE IRON PARTICLES LASER EVAPORATED IN A CONTROLLED OXYGEN ATMOSPHERE

T. Turkki, B.J. Jönsson, V. Ström, H. Medelius*, M.S. El-Shall, K.V. Rao**

Department of Condensed Matter Physics, Royal Institute of Technology, S-100 44 Stockholm, Sweden
* Department of Ceramics, Royal Institute of Technology, S-100 44 Stockholm, Sweden
** Department of Chemistry, Virginia Commonwealth University, Richmond VA 23284-2006

Abtract--Magnetic nanoparticles of iron and iron oxide have been prepared in a modified upward thermal diffusion cloud chamber using pulsed laser evaporation. SEM/TEM studies of these particles reveal a size distribution with a mean diameter of about 60 Å. FTIR spectrum measurements are used to investigate the difference in oxidation level between nanoparticles prepared at different partial oxygen pressures. The complex magnetic behaviour of these particles was studied using DC- and AC-susceptibility measurements. All samples exhibit superparamagnetism with blocking temperatures ranging from 50 K to above room temperature. The coercivity fields as well as the dependence of the blocking temperature on measuring frequency have been studied. Magnetic anisotropy constants are found to be one order of magnitude higher than is known for the bulk values. The mean particle size estimated from the magnetic data is found to be in perfect agreement with the TEM observations.

I. INTRODUCTION

Ultrafine- or nanoparticles, have been the subject of intense research in recent years. Nanoparticles have unique properties in comparison with the bulk: large surface to volume ratio, discrete electron energy levels which can be easily tuned over a wide range of compositions, etc. They often exhibit completely new phenomena offering new challenges for technological applications. The surface characteristics of the nanoparticles are dependent on details of the preparation technique. These properties can in turn greatly affect the final properties of the material like ability to build larger cluster structures and the oxidation of the surface. The purity of the material also depends on the preparation technique. It is generally believed that a higher purity is obtained in gas phase reactions than in solution reactions. [1,2]

Magnetic nanoparticles become single domain below a certain size and exhibit superparamagnetism and quantum tunnelling of magnetization. Interest in magnetic nanoparticles remains high because of the wide range of potential applications, including information storage, ferrofluids, permanent magnets and pigments in paints. Iron oxide nanoparticles can also have advanced properties as catalysts. In this paper we present the magnetic properties of iron and iron oxide nanoparticles produced by pulsed laser evaporation in the presence of different oxygen partial pressures. Their magnetic properties are analyzed in terms of superparamagnetism.

II. EXPERIMENTAL

Iron oxide samples were prepared in a modified upward thermal diffusion cloud chamber. A sketch of the chamber is shown in figure 1. The iron target was set on the bottom plate. The chamber was filled with desired amount of oxygen and then further filled with helium to 800 torr. Top plate was cooled down to -100 °C with liquid nitrogen and the bottom plate was at room temperature. Metal was vaporized using Nd:YAG laser (532 nm, 20 Hz and 20 mJ/pulse). The details of the method are described elsewhere [3]. In the presented investigations the partial oxygen pressure was varied from 0 to 500 torr and the total pressure was kept at 800 torr in all experiments.

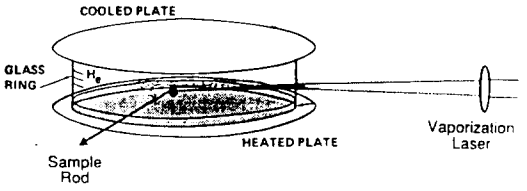

Fig. 1 A sketch of the diffusion cloud chamber [4].

SEM and TEM micrographs were taken with JEOL SM 840 and JEOL 2000 EX instruments, respectively. In TEM the electron diffraction patterns were taken to identify the structure.

The infrared absorption spectra were recorded on a Nicolet 750 Magna Fourier transform spectrophotometer. Absorption was measured in the energy range of 400 - 4000 cm^{-1} with 4 cm^{-1} resolution. 64 scans and background scans were collected. KBr (170 mg) and sample (0.3 -1.7 mg) were grained and then pressed to pellet at 8 tons pressure. The sample chamber was purged with dry air for 10 - 20 min. before scanning. Measurements were done under atmospheric pressure.

DC magnetic measurements were performed using Quantum $MPMS_2$ SQUID magnetometer. The zero field cooled measurements were performed by cooling the sample to 5 K at zero field and then applying 20 G field for the warming up scan. Hysteresis loops were measured at selected temperatures. Between every loop the sample was warmed up to 300 K and using the oscillation mode the remanence field was minimized. AC magnetic measurements were performed using a home-built two-

position AC-susceptometer with a three-coil mutual-inductance-bridge. The driving field was 3 Oe for all measurements and the frequency was varied from 4 Hz to 4 kHz.

III. RESULTS AND DISCUSSION

A. Structure and morphology

For brevity we label the samples Fe-0, Fe-10... letting the number denote the partial oxygen pressure, in torr, during preparation. The color of the samples goes from very dark brown, almost black (the color of FeO and Fe_3O_4) to reddish brown (the color of γ-Fe_2O_3) with increasing oxygen pressure. SEM/TEM micrographs were used to study the particle morphology. TEM bright field images showed the samples to consist of very small particles with mean diameter of about 60 Å. Some bigger particles with size 50 - 500 nm were also present. No significant difference in particle size distribution was observed between different batches of samples. The size of the particles is found to be controlled by the total pressure, temperature gradient and the partial pressure of the metal vapor. These parameters were kept the same for every preparation.

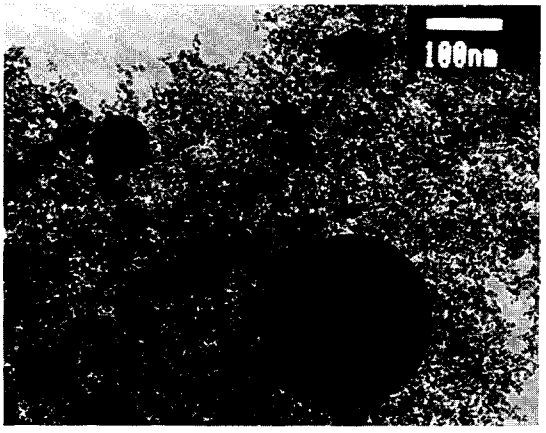

Fig. 2. TEM micrograph of sample Fe-10.

The diffuse electron diffraction patterns indicate the presence of FeO, Fe_3O_4 and γ-Fe_2O_3 phases. The diffraction patterns from different samples were much the same. In particular, no lines indicating α-Fe were observed in the Fe-0 sample. This could arise from the Fe core being very small or having an amorphous structure and hence showing very broad lines.

In fig.3 we show the infrared absorption spectra for two of our samples. The nanoparticles have a very high surface to volume ratio. As a consequence the adsorption of the surface species can compete with the ones in the bulk. All surfaces are more or less hydrolyzed, thus water molecules from ambient atmosphere can easily adsorb on the OH surface groups. The absorption at 3400 cm^{-1} and at 1640 cm^{-1} are due to stretching and bending vibrations of water adsorbed on the surface of the sample. Samples also have contamination of atmospheric CO_2 chemisorbed on the surface. The absorption at 1380, 1420 and 1560 cm^{-1} are related to these CO_3^{2-} species. The 1360 cm^{-1} band, which is narrower than the other ones, is associated with carbonate species on the basic surface site, i.e. the ν_1-vibration of the linearly adsorbed CO_2. The amount of CO_2 adsorbed is found to be much bigger for sample Fe-500 confirming the higher oxidation of this sample.[5]

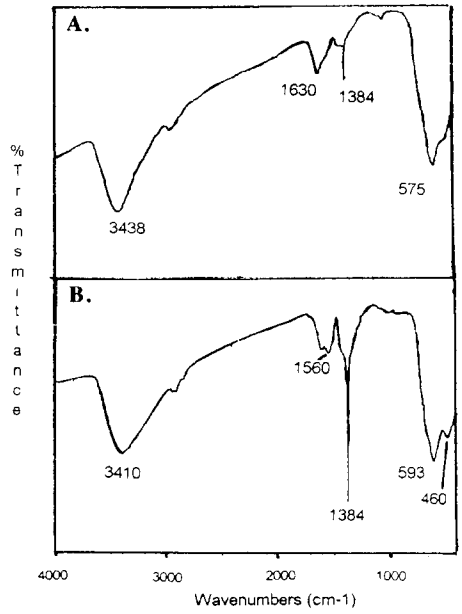

Fig. 3. FTIR spectrum of samples Fe-0 (a) and Fe-500 (b).

At lower oxygen pressures the samples are found to consist mainly of Fe_3O_4 with some γ-Fe_2O_3 contamination. The γ-Fe_2O_3 peak at 450 cm^{-1} is barely visible. At high partial oxygen pressures samples seem to be close to the γ-Fe_2O_3 form. The broadness of the bands at 590 and 450 cm^{-1} is due to a quasi-amorphous state. [6]

B. Magnetics

Magnetic measurements on the same nanoparticles give complementary information about their structure and composition. The saturation magnetization M_S was determined from M/H measurements up to 9 kOe, plotted as M vs 1/H and then extrapolated to infinite fields. M_S was about 20 emu/g for all the samples, which is one order of magnitude smaller than the bulk value for Fe (220 emu/g) and its oxides (80 emu/g). The temperature dependence of the magnetization is well fitted by Bloch's $T^{3/2}$ law:

$$M = M_s\left(1 - bT^{3/2}\right) \quad (1)$$

where b is Bloch's constant ($3*10^{-6}$ $K^{-3/2}$ for bulk Fe). In our case b is found to be $3*10^{-5}$ $K^{-3/2}$ for Fe-0 and about $5*10^{-5}$ $K^{-3/2}$ for the other samples, i.e. one order of magnitude higher than the value for the bulk. Similar differences in M_S and in the temperature dependence have been found by other groups, for very small Fe particles as well as for other systems [7,8]. Both differences are related to the very high surface to volume ratio. Surface layers may be nonmagnetic or they may also experience spin canting [9]. Theories also show that b of the surface can be 2-3.5 times larger than b of the interior, due to larger fluctuations of the surface moments [10].

The iron and iron oxide particles prepared in this study, have sizes within the single domain particle regime (about 200Å for Fe). Their magnetic behaviour is well described in terms of superparamagnetism which appears when the anisotropy energy barrier $\Delta E=KV$ that must be overcome before a particle can reverse its magnetization, is smaller than the thermal energy k_BT. Thermal fluctuations will thus cause the magnetization direction to fluctuate randomly between the easy directions. In an applied field an ensemble of single domain particles will behave as a paramagnet with a huge moment $\mu=M_sV$, hence the term *superparamagnetism* coined by Bean [11].

The superparamagnetic relaxation time τ is given by

$$\tau = \tau_0 e^{KV/k_BT} \quad (2)$$

where τ_0 is of the order of 10^{-9} s [12]. The superparamagnetic behaviour is observed above the blocking temperature, T_B which will depend on the measuring time scale of the experiment. Below T_B the particles are magnetically frozen and hysteresis will appear.

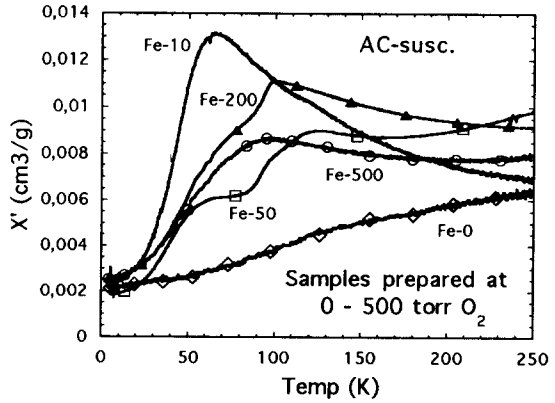

Fig.4 In-phase AC susceptibility as a function of temperature.

The in-phase AC susceptibility χ' for five samples prepared at different partial oxygen pressures, is shown in Fig.1. χ' increases monotonically with temperature for Fe-0 and no cusp is observed below 300K. This behaviour is expected since a blocking temperature of 300K corresponds to iron particles 60-80 Å in size [7]. When the particles consist of iron oxide instead of iron, there is a dramatic change in behaviour. A clear cusp is seen at about 65K in sample Fe-10. Increasing the oxidation of iron, as in Fe-50, gives rise to another cusp around 110 K which then dominates in Fe-200. Finally, this is the only cusp seen in Fe-500.

To further point out the significance of the blocking temperature, we measured the coercivity field as a function of temperature for three of our samples. There is a clear increase in coercivity, starting at the blocking temperatures 50K, 100K and above room temperature respectively. The coercivity does not fall to zero above T_B as it should for a purely superparamagnetic sample. Probably this is because of the existence of some bigger particles (50-500nm, seen in the TEM pictures) as well.

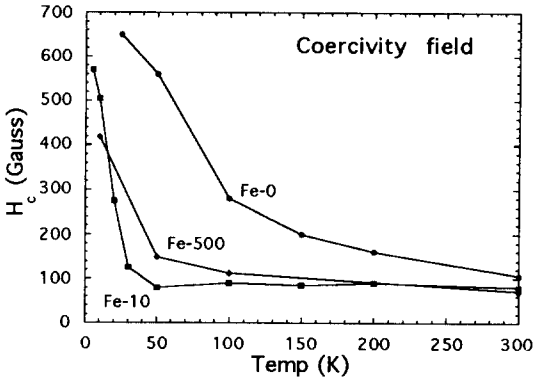

Fig.5 Coercivity field as a function of Temperature for samples showing one single cusp.

The magnetization of a paramagnet follows a Langevin function:

$$\frac{M}{M_s} = L(a) = \coth a - \frac{1}{a} \quad , \quad a = \frac{\mu H}{k_BT} \quad (3)$$

This dependence is also true for a purely superparamagnetic material with particles all having the same size [13]. In a general case there is always a size distribution but since the Langevin function is a linear function for small arguments, $L(a)\approx a/3$, this will hold even for a distribution of particle sizes. Thus, measuring M/H-loops and taking the slope around zero field gives us a means of calculating the mean magnetic moment of our particles and hence a mean particle diameter.

The mean magnetic moment per particle for sample Fe-10 is found to be 5100 μ_B. Assuming the dominate phase to be Fe_3O_4, which has 4.1 μ_B per molecule, eight molecules per unit cell and a lattice constant of 8.39 Å, we get a mean particle diameter of 60 Å. This is in remarkable agreement with the TEM observations.

Knowing the mean volume of our particles we can now estimate K_1. If the cusp in χ' originates from blocking of superparamagnetism, its peak should shift as a function of the measuring time, i.e. the inverse of the driving frequency. We measured χ' at six different frequencies between 4 and 4000 Hz and included a SQUID measurement with a measuring time of about 100 s. Taking the maximum of χ' to be the blocking temperature and plotting $1/T_B$ vs ln(f), f being the driving frequency, we get a straight line (Fig.3). The slope of this line is equal to $-k_B(|K_1|V)^{-1}$, according to eq.(1).

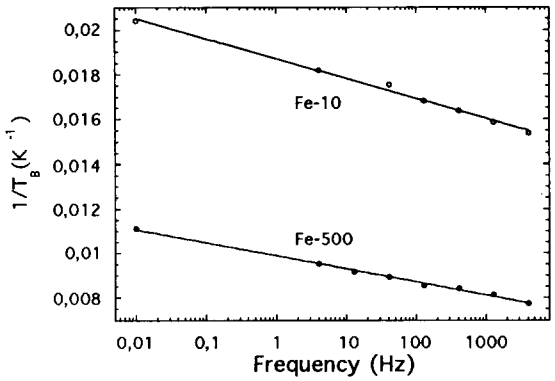

Fig.6 Plot showing the blocking temperature as a function of measuring frequency for samples Fe-10 and Fe-500. The agreement with a superparamagnetic behaviour is obvious.

In the case of a cubic structure with the easy direction in the <111> direction, K_1 is replaced by $K_1/12$ [13]. We thus get an anisotropy constant of $|K_1|=2.1*10^6$ ergs/cm^3 for sample Fe-10. If we assume the mean size to be equal in all samples we get $|K_1|=3.1*10^6$ ergs/cm^3 for sample Fe-500. This is one order of magnitude larger than the bulk value for Fe_3O_4 and γ-Fe_2O_3 but agrees very well with values found for small particles by other groups [14].

These calculations can now help us to explain the trend seen in Fig.4. Since all samples have about the same size distribution it is the difference in composition that determines the different magnetic behaviour. The high blocking temperature of sample Fe-0 is consistent with an iron core and an outer shell of iron oxide since the anisotropy barrier is higher for iron than for its oxides. It is higher because in iron the easy directions are along the cube sides <100> and K_1 should be replaced by $K_1/4$ and not $K_1/12$ [13]. When the core is Fe_3O_4 the anisotropy barrier is reduced and the blocking temperature falls to about 50 K. With increasing oxidation, the fraction of γ-Fe_2O_3 increases and since its anisotropy barrier is slightly higher than that for Fe_3O_4, a new cusp develops at about 110 K. As the γ-Fe_2O_3 further increases this cusp starts to dominate and finally is the only one observed in sample Fe-500.

IV. CONCLUSIONS

In conclusion we have demonstrated a simple technique to prepare nanoparticles of iron and iron oxide. The particles composition has been studied and their magnetic properties have been analysed in terms of superparamagnetism. By varying the partial oxygen pressure during preparation we have been able to change the oxidation state of Fe. Particles prepared at low oxygen pressure consist mainly of FeO and Fe_3O_4 while those prepared at higher oxygen pressure consist of γ-Fe_2O_3. As a consequence the magnetic behaviour changes in a rather complex way, going from low oxygen pressure to higher. The magnetic properties are found to be consistent with the implications from the particle size and structure. Magnetic anisotropy constants calculated from our experimental data agree well with the expected values for small particles.

ACKNOWLEDGEMENT

It is a pleasure to acknowledge many valuable discussions with Prof. Dan E. Dahlberg during his visit with us. T. Turkki is most obliged to colleagues at the Dept. of Chemistry at VCU for their hospitality and financial support during her stay at VCU. This research has been partially supported by the Swedish National Cluster Consortium, and NSF Grant CHE 9311643 and the Petroleum Research Fund (2764-AC), in USA.

REFERENCES

[1] Siegel, R.W. *Annu. Rev. Mater. Sci.* **21** ,559 (1991).
[2] Kaatz, F.H., Chow, G.M. and Edelstein, A.S., *J. Mater. Res.* **8** 995 (1993).
[3] El-Shall, M.S., Slack, W., Vann, W., Kane, D. and Hanley, D., *J. Phys. Chem.* **98**, 3067 (1994).
[4] El-Shall, M.S., Slack, W., Vann, W., Hanley, D.and Kane, D, *Mat. Res. Soc. Symp. Proc.*, Vol. 351, 369 (1994).
[5] Ramis, G., Busca, G. and Lorenzelli, V., *Mater. Chem. and Phys.* **29**, 425(1991).
[6] Baraton, M-I.,*unpublished results.*
[7] Gangopadhyay, S., Hadjipanayis, G.S., Dale, B., Sorenson, C.M., Klabunde, K.J., Papaefthymiou, V., and Kostikas, A., *Phys. Rev. B* **45**, 9778 (1992).
[8] Yamada, H., Takani, M., Kiyama, M., Takada, J. Shinjo, T. and Watanabe, K., *Adv. Ceram.* **16**, 169 (1985).
[9] Haneda, K. and Morrish, A. H., *IEEE Trans. Magn.* **25**, 2597 (1989).
[10] Mills, D. L., *Commun. Solid State Phys.* **4**, 28 (1971).
[11] Bean, C.P. and Livingston, J. D., *J. Appl. Phys* **30**, 120S (1959).
[12] Néel, L., *Ann. Geophys.* **5**, 99 (1949).
[13] Cullity, B.D., *Introduction to Magnetic Materials* (Addison-Wesley, Reading, MA, 1972), p. 410-418.
[14] Mørup, S. and Topsøe, H., *Appl. Phys.* **11**, 63 (1976).